Asymmetric Silver to Oxide Adhesion in Multilayers Deposited on Glass by Sputtering

E. Barthel [a] , O. Kerjan [a], P. Nael [a] and N. Nadaud [b]

[a] *Unité Mixte CNRS/Saint-Gobain " Surface du Verre et Interface ", Saint-Gobain Recherche, BP 135, F-93303, Aubervilliers, Cedex, France.*

[b] *Saint-Gobain Recherche, BP 135, F-93303, Aubervilliers, Cedex, France.*

Abstract

We have developed a wedge-loaded double-cantilever beam adhesion measurement set-up for thin films deposited on glass by sputtering. The test is described in details. Results on the Glass/sublayer/Ag/ZnO multilayer provide evidence that SnO_2 or TiO_2 perform better than ZnO as a sublayer. Then however, rupture within the multilayer shifts to the upper Ag/ZnO interface. The latter is shown to be tougher than the lower ZnO/Ag interface, an asymmetry due to non-equilibrium interfacial structures.

Key words: Adhesion, Silver, Sputtering, Zinc Oxide

PACS: 68.35.G, 68.55

Email address: etienne.barthel@saint-gobain.com (E. Barthel).

1 Introduction

Thin film multilayers deposited on glass are widely used for flat optical, photoelectric and electrochromic devices. Typical applications are Infra-Red filters against heat-generating solar radiations (solar control), solar cells for electrical power generation or voltage-controlled devices for tunable absorption in the visible light frequency range. For instance, in the present paper, we consider a ZnO/Ag/ZnO sandwich, with respective layer thicknesses of 20, 10 and 20 nm. This stack stands as a prototype both for solar control coatings [1] and for solar cell electrodes [2].

In the metal/oxide adhesion literature, the metals are classified according to their ability to react with the oxide and form an interphase. Silver, along with gold and platinum belongs to the group of non-reactive metals [3] which form an abrupt interface with all oxides, without interphase. The resulting adhesion energies are low. In many applications, however, adhesion is a crucial issue. This is the case for instance when mechanical strength is required for further processing or for integration in complex systems. Scratch resistance is also a general concern either during process or during service.

Assessment of the adhesion of such thin films is therefore necessary. Although more academic approaches such as high temperature sessile drop methods are useful to grasp some of the underlying mechanisms, they cannot take into account all the specifics of adhesion within a multilayer: such characteristics as stoechiometry or structure are largely dependent upon the deposition conditions. Therefore, for thin films, one of the primary requirements is to measure the adhesion directly on the system under study.

For that purpose, we have developed a set-up to measure the adhesion energy of multilayer films in the tens of nanometer thickness range deposited by RF sputtering on thick glass substrates. In the present paper, the effect of modifications or substitutions of the lower ZnO layer in ZnO/Ag/ZnO stacks (Fig. 1) was investigated. The relative performance of Si_3N_4, ZnO and SnO_2 are compared. The crack path selection mechanism is discussed. Through the adhesion measured in this way, we also evidence more complex phenomena: in particular, we show directly that deposition of the metal on top of the oxide does not result in the same work of adhesion as deposition of the same oxide on top of the same metal. The work of adhesion is also shown to depend upon the next nearest layers, *i.e.* layers which are not directly adjacent to the interface of rupture.

2 Experimental details

2.1 The layers

The systems studied here were deposited on the glass substrate by magnetron sputtering using an Alcatel Lina350 in-line sputtering system. The typical stack (Fig. 1) is Glass/sublayer (20)/Ag (10)/ZnO (20) where the figure in brackets is the layer thickness in nanometers. The stack is terminated by a Si_3N_4 layer of thickness varying between 4 and 35 nm. A number of sublayers such as ZnO, SnO_2 and Si_3N_4 were tested. ZnO and SnO_2 were obtained by reactive sputtering of respectively Zn and Sn planar targets using argon and oxygen as primary sputtering and reactive gases. All the layers within the multilayer are deposited in-line, without breaking the vacuum, with a

pre-sputter time of 3 minutes. Si_3N_4 was obtained by reactive sputtering of a polycrystalline Si target using argon and nitrogen as primary sputtering and reactive gases. Ag was obtained by sputtering an Ag planar target using argon as sputtering gas. For all the experimental runs, the background pressure before deposition was about 7.10^{-7} mbar and the total sputtering pressure was 8.10^{-3} mbar. The cathodic power applied to the targets was 200 and 2000 W for Ag and dielectric materials, respectively. For reactive sputtering, oxygen and nitrogen partial pressures were adapted for a full oxidation or nitridation of the SnO_2, ZnO or Si_3N_4, respectively. All substrates were cleaned by hot demineralized water and mechanical brushing.

2.2 Adhesion energy measurements - The Double Cantilever Beam test

The literature on thin film adhesion energy measurements is wide [4,5,6,7,8]. This results from the fact that many measurement set-ups are specific to a given film-substrate combination. The applicability of a given method will depend, among other parameters, upon the thickness of the layer, the respective mechanical properties of the layer and the substrate, the relevant crack velocity.

For thin films, a number of experimental set-ups, which are easy to implement, such as the scratch test or the pull-out test, return qualitative rather than quantitative results. For more quantitative measurements, it is necessary to apply the mechanical stress with the help of a backing of some sort. Here, the backing is made out of glass: in our cleavage set-up, two glass plates, one of them bearing the multilayer, are glued together (Fig. 2 a). Cleavage of such a sandwich is a complex physico-mechanical process which involves dissipation

through irreversible processes. In such cases, the interfacial toughness G (*i.e.* the measured work of adhesion) can often be expressed as

$$G = w\phi \tag{1}$$

where w is the thermodynamic work of adhesion for reversible surface separation and ϕ expresses the enhancement of the work of adhesion due to irreversible processes. Extraction of the thermodynamic work of adhesion from the interfacial toughness is seldom straightforward [9,10]. This extraction will not be attempted here. However, we will assume that the enhancement factor ϕ is constant and the test will only be used to compare thermodynamic work of adhesion through the interfacial toughness.

2.2.1 Description of the test

A glass backing identical to the 2.3 mm float glass substrate is glued onto the thin film. Typical samples are 70 mm long and 50 mm wide. The glue is Epotecny 505, a two-components epoxy which was prepared as specified by the manufacturer and cured at 80°C for 45 min. The glue layer is about 25±5 μm thick, with a 2 GPa Young's modulus. The multilayers are stable to at least 300 ° C, in particular without silver dewetting, suggesting they are unaffected by the thermal treatment. No trace of glue diffusion within the multilayer was observed by X-ray photoelectron spectroscopy (XPS).

The cleavage of the sample is obtained by the gradual introduction of a bevelled blade. The blade is mounted on an electric jack, which allows for precise positioning. In this way, the opening displacement δ of the arms of the DCB sample can be controlled (Figure 2 a): the typical opening lies in the 30 μm

to 250 μm range. It is measured by a high magnification camera (Figure 2 b).

In this way, the test is conducted at fixed grip and is mechanically stable, *i.e.* catastrophic rupture is avoided and the crack length can be increased in a controlled manner. As a result, the following experimental procedure is used: for a given sample, the opening is gradually increased and for each value of the opening, the crack length L – typically 2 to 4 cm – is measured with a transparent ruler. Due to viscous relaxation in the glue, it takes a few minutes for the crack position to stabilize. A typical waiting time of 15 min is allowed for between each opening increment. The test is conducted at ambient air.

2.2.2 Crack propagation control

Careful sample preparation is crucial to prevent surface flaws from propagating into the glass and ruining the sample. For that purpose, after curing the glue, the sample is carefully re-cut into its final rectangular shape so as to remove glue spill-outs. At this stage, flaws on the glass edges should be avoided or suppressed by polishing so as not to compromise the overall sample strength. Of course, crack initiation must take place within the multilayer. For that purpose, release layers may be avoided if in the final re-cutting step one of the small sides of the sample is cut into a pointed end (Fig. 2 b); pre-cracking is then achieved by pressing the blade onto the glue joint at the tip edge. In the systems studied here, this results in crack initiation: wherever it started, this initial crack soon propagates into the multilayer where it stabilizes at a definite interface. With this crack initiation procedure, a broader range of samples is suitable for adhesion measurements, including those where a release layer cannot be provided for.

2.2.3 Locus of failure

Identification of the locus of failure is of primary importance for attribution of the adhesion energy measured to a specific interface and also for assessment of the nature of the crack propagation. It is achieved by XPS (CLam 2, Fisons Instruments, Mg Kα) of both cleavage surfaces. In the present systems, perfectly interfacial ruptures at a definite interface within the multilayer have always been found, with negligible material transfer on the opposite surface, as illustrated on Fig. 3. This is confirmed by the very low roughnesses (less than 1 nm RMS over 1 μm^2) measured after cleavage by Atomic Force Microscopy (AFM).

2.2.4 Data interpretation

There are two steps in the data interpretation. The first one is to calculate the interfacial toughness from the cleavage data. This depends on the mechanics of the glass arms, is relatively straightforward and is detailed in this section. The next step is to make a connection between the mechanics of the test – *i.e.* geometry, material properties and interfacial toughness – and the decohesion process at the interface. This step involves a mechanical description at the scale of the glue layer and is much more involved. It will not be attempted here in any detail: we will only argue later in the discussion that a simple monotonic relation between interfacial toughness and thermodynamic work of adhesion holds and that rupture occurs at the weakest interface.

The interfacial toughness is derived from the data through the standard augmented beam model by Kanninen [11]. However the elastic foundation contribution is actually negligible even when the glue layer is taken into account [12],

so that the simplest beam theory [13] would be adequate. According to the augmented beam model

$$G = \frac{3Eh^3\delta^2}{16(L+0.6h)^4} \tag{2}$$

where δ and L are the crack opening and crack length, and E and h the beam Young's modulus and thickness, and G is the energy release rate. Indeed, beam bending stores elastic energy. The energy release rate G is the amount of elastic energy released upon incremental crack advance. At mechanical equilibrium, it is equal to the toughness of the adhesive joint. In turn, there is a relation between this interfacial toughness and and the thermodynamic work of adhesion of the interface of rupture. This relation will be discussed below.

3 Results

Typical results plotted according to Eq. 2 are displayed in Fig. 4. The linear plots confirm the applicability of the Kanninen model. Good repeatability from sample to sample is also evidenced by the superimposition of the data. The results for the various sublayer substitutions are summarized in the Table. The interface of rupture as identified by XPS is denoted by a // in the stack description.

A Si_3N_4 sublayer (system 1) results in the weakest joint. Rupture occurs between Si_3N_4 and silver. ZnO (system 3) improves on Si_3N_4, but ZnO on Si_3N_4 (system 2) is not as good as bare ZnO. In these last two cases, rupture is located between the *lower* ZnO layer and silver. TiO_2 (system 4) and above all SnO_2 (system 5) perform significantly better than ZnO. Then, however

cohesion fails between silver and the *upper* ZnO layer.

4 Discussion

4.1 Relation between interfacial toughness and thermodynamic work of adhesion

Comparison of the interfacial toughness values measured here with typical metal/oxide adhesion energies measured by the sessile drop technique suggest that our values overestimate the adhesion energy. For instance, a representative value for the adhesion energy of silver on a large gap oxide like sapphire is 0.34 Jm^{-2} [14]. Since silver obviously dewets on Si_3N_4, we would expect the adhesion energy in this case to be lower, of the order of 0.15 - 0.3 Jm^{-2}.

As expected, the difference between the interfacial toughness and the thermodynamic work of adhesion values demonstrate that the elastic energy release rate measured includes additional effects. This is where the details of the mechanics of the system at the local scale have to be considered. A first kind of effects result from residual stresses in the layers. They are expected to be of small magnitude for such thin layers in a cleavage geometry (appendix A.1). To explain an enhancement of the adhesion, additional mechanical dissipation processes are invoked. Since the rest of the system is essentially brittle (glass) or negligibly thin (silver), this dissipation most likely takes place within the glue layer. A sizeable viscoelastic contribution is ruled out because the tests are conducted at virtually zero crack tip velocity. The source of dissipation is plastic deformation in the glue: more details may be found in appendix A.2. In brief, we assume the plastic dissipation takes the form of an enhancement

factor which is more or less constant in the adhesion energy range considered here.

4.2 Interfaces within the multilayers - Adhesion

4.2.1 The Lower Interface

For non reactive metals like silver, the adhesion to oxides is still not well understood. The difficulty arises from the fact that several effects may contribute to the – low – final value. A short and recent review may be found in ref. [15]. General trends have been experimentally identified such as decreasing adhesion with increasing oxide gap [16] or increasing adhesion with increasing enthalpies of mixing [17].

Along these lines, the reduction of adhesion when Si_3N_4 is substituted for ZnO can be rationalized at least in two ways: a larger gap and a smaller metal/nitrogen than metal/oxygen affinity.

The reduction of adhesion when the ZnO layer is deposited on top of a Si_3N_4 sublayer signals intrinsic multilayer issues: the nature or structure of the next nearest layer influences the interface. Indeed, the Si_3N_4 layers are significantly rougher than the bare glass substrate. Along with surface chemistry, this forms a possible reason to alter the growth of the subsequent ZnO layer, which then offers a lower interfacial energy to silver.

4.3 Crack path selection

Our data show that SnO_2, and also TiO_2, provide a more adhesive substrate to silver than ZnO. The latter is hygroscopic so that environmental conditions and water assisted corrosion may be crucial here. Moreover, the crack path changes when ZnO is replaced by one of theses oxides. This means that the toughness then measured is actually the toughness of the upper Ag/ZnO interface.

Before comparing the relative interfacial toughnesses, the crack path selection mechanism should be discussed. Crack path selection is a non trivial issue in the case of the bi-material sandwich we use because crack propagation on one side of the glue layer breaks the symmetry so that the details of the stress field at the crack tip (mode mixity) may induce crack deviations [18].

Elastic calculations [19,20], which are valid in the present case provided the plastic zone is not too large, suggest that the glass/epoxy system lies on the borderline between stable growth within the layer and propagation close to the interface. In the present case, we may also rely on the aluminum/epoxy data: indeed the elastic properties of glass and Aluminum are very close. In fact, in the Aluminum/epoxy sandwiches, calculations predict a small negative value of the phase angle (around -13 °) [18] while experimentally it is observed that with a symetrical loading, rupture occurs in the middle of the epoxy layer, despite the higher toughness [18]. To sum up, in Fig. 1, we expect a weak tendency for crack deviation upwards, towards the more compliant part.

However, rupture at the interface is observed here. This is likely to occur if the interfacial energy is substantially smaller than the cohesion energy of the glue

(a few hundred J/m^2). In our case, it is this energy criterion which primarily controls the crack path.

However, the crack deviation mechanism should be kept in mind when the question of the crack path selection *within* the multilayer arises. An interesting perspective in the present experimental set-up is set by the possibility of tuning the asymmetry of the stress field at the crack tip by the asymmetry of the glass arms of the DCB. Hopefully, the crack propagation, and thus the interface of rupture within the multilayer could be controlled in this way.

4.3.1 The Upper Interface: Asymmetry

In brief, we have observed that: 1) on the ZnO/Ag/ZnO stack, the crack always propagates at the lower interface, although the mode mixity tends to drive it upwards, to the glue layer; 2) when the crack propagates at the upper Ag/ZnO interface, the interfacial toughness is larger than when it propagates at the lower.

The simplest scenario is that the *thermodynamic work of adhesion* of the upper interface is actually larger than the lower, thus driving the crack to the lower interface. An alternative explanation is that the increased adhesion energy at the upper interface is due to an increase in plastic dissipation because of the reduced thickness of the top elastic layer. However, this is not the case since the same behaviour is observed with thicker upper layers, increasing the top Si_3N_4 layer to 35 nm.

In both cases, we conclude that the thermodynamic work of adhesion for the SnO_2/Ag and TiO_2/Ag interfaces is at least as large as for the Ag/ZnO

interface. This means that substituting SnO_2 or TiO_2 for ZnO results in at least about a 50% increase. This is not due to roughness effects because the SnO_2 and ZnO layers have similar roughness. However, it is consistent with the observation that non-reactive liquid metals wet TiO_2 but not ZnO [3].

The asymmetry between the ZnO/Ag and Ag/ZnO adhesion is surprising at first sight because the *equilibrium* expression for the adhesion energy, the Young's equation, is symmetric with respect to the materials involved. However, during the growth of the layer, equilibrium is not reached. This is illustrated by the high temperature dewetting of silver films on oxide substrates. Several factors like adatom diffusion or spreading pressure will differ for Ag on ZnO or ZnO on Ag deposition. The resulting structure of the interface and therefore the adhesion energies will then be different. A similar case of asymmetric interfaces appear in the Mo/Si multilayers developped for EUV reflective optics [21].

5 Conclusion

We have applied the wedge controlled DCB test to thin multilayers deposited on glass by sputtering. A specific sample preparation and experimental procedure allow for reliable measurements. In terms of adhesion of the silver layer, the effect of the nature of the sublayer has been quantified:Si_3N_4, ZnO, TiO_2 and SnO_2 exhibit increasing performances. For the last two, the crack path switches to the upper Ag/ZnO interface, the adhesion energy of which is actually the measured quantity. We provide evidence that this upper Ag/ZnO is stronger than the lower ZnO/Ag. This asymmetry is due to the non equilibrium configurations of these otherwise identical interfaces. Next-nearest layers

also play a role in the adhesion.

6 Acknowledgements

We thank J. Jupille for interesting discussions.

References

[1] E. Ando and M. Miyazaki, Thin Solid Films 392 (2001) 289.

[2] S. Ray, R. Das and A.K Barua, Solar energy materials and solar cells 74 (2002) 387.

[3] A. M. Stoneham, Applications of Surface Science 14 (1983) 249.

[4] P. Y. Hou and A. Atkinson, Materials at high temperatures 12 (1994) 119.

[5] M. D. Drory and J. W. Hutchinson, Proc. Royal Soc. A 452 (1996) 2319.

[6] A. G. Evans, J. W. Hutchinson and Y. Wei, Acta mater. 47 (1999) 4093.

[7] K. L. Mittal (Ed.), Adhesion Measurement of Films and Coatings, vol. 2, VSP International Science Publishers, Zeist, The Netherlands, 2001.

[8] A. A. Volinsky, N. R. Moody and W. W. Gerberich, Acta Mater. 50 (2002) 441.

[9] R. A. Schapery, Int. J. Fract. 39 (1989) 163.

[10] S. Wei and J. W. Hutchinson, Int. J. Fract. 95 (1999) 1.

[11] M. F. Kanninen, Int. Jour. of Fracture 9 (1973) 83.

[12] F. E. Penado, J. Composite Mater. 27 (1993) 383.

[13] J. W. Obreimov, Proc. Roy. Soc. A 127 (1930) 290.

[14] D. Sotiropoulou, S. Agathopoulos and P. Nikolopoulos, J. Adhesion Sci. Technol. 10 (1996) 989.

[15] C. T. Campbell and D. E. Starr, J. Am. Chem. Soc. 124 (2002) 9212.

[16] J. G. Li, Compos. Interfaces 1 (1993) 37.

[17] R. Sangiorgi, M. L. Muolo, D. Chatain and N. Eustathopoulos, J. Am. Ceram. Soc. 71 (1988) 742.

[18] J. S. Wang and Z. Suo, Acta Metall. Mater. 38 (1990) 1279.

[19] N. A. Fleck, J. W. Hutchinson and Z. Suo, Int. J. Solids Structures 27 (1991) 1683.

[20] R. O. Ritchie, R. M. Cannon, B. J. Dalgleish, R. H. Dauskardt and J. M. McNaney, Mat. Sci. Eng. A166 (1993) 221.

[21] S. Yulin, T. Feigl, T. Huhlmann, N. Kaiser, A. I. Fedorenko, V. V. Kondratenko, O. V. Poltseva, V. A. Sevryukova, A. Yu. Zolotaryov and E. N. Zubarev, J. Appl. Phys. 92 (2002) 1216.

[22] R. H. Dauskardt, M. Lane, Q. Ma and N. Krishna, Eng. Fract. Mech. 61 (1998) 141.

A The mechanics of the test

A.1 Intrinsic stresses relaxation

Such layers as ZnO or Si_3N_4 may store significant residual stresses. Their contribution to the thermodynamic work of adhesion will depend upon stress sign and test geometry. However, it is expected that in such confined geometries, minute film deformations are allowed, so that very little of these stresses relax

upon crack propagation [22]. As a result, residual stress contributions to the measured energy release rates will not be considered here.

A.2 Plastic dissipation

Assuming that the glue and glass Young's modulus are respectively 2 and 70 GPa, and that the glue yield stress is in the 30 to 100 MPa range, a plastic zone size of roughly 1 - 10 μm can be estimated [10]. This result means that confinement of the plastic zone by the glass backing is not essential. This is essentially due to the low adhesion energies encountered in the present systems. As a result, the thickness of the glue layer is not a first order parameter. It would be tempting to try and calculate the enhancement factor relating interfacial toughness and thermodynamic work of adhesion. Unfortunately, this would require extensive finite element analysis, taking into account the complex tensile behaviour of the epoxy glue and the thickness of the residual layer between fracture plane and glue (Fig. 5). It is therefore possible, but was not undertaken here.

We only assume that the larger the thermodynamic work of adhesion, the larger the interfacial toughness. Thus, by comparing toughnesses, we compare thermodynamic works of adhesion indirectly.

Captions

Table

Table: interfacial toughness for different multilayers as measured with the wedge-loaded DCB test with a glued glass backing. The interface of rupture is denoted by the // sign.

Figures

Fig. 1: Schematics of a typical multilayer. Layer thicknesses are in the 10-20 nm range. In this example, the sublayer (between the glass substrate and the silver layer) is ZnO.

Fig. 2: Schematics of the cleavage set-up: a) side view: the wedge controled opening δ and the crack length L are measured and the interfacial toughness calculated with the Kanninen model (Eq. 2); b) top view: end cut for crack initiation, showing also the position of the blade; the arrow indicates the position where the opening δ is masured.

Fig. 3: Typical XPS spectra of the cleaved surfaces for a substrate/ZnO/Ag/ZnO/backing stack. The rupture, which occurred between the silver layer and the ZnO on the substrate side (glass), is almost perfectly interfacial, with negligible material transfert.

Fig. 4: Typical data plot according to the Kanninen model. The slope is proportional to the interfacial toughness G (Eq; 2). The points where collected from respectively two and three samples for the high adhesion (filled symbols)

and low adhesion (empty) samples.

Fig. 5: Schematics of the mechanics of crack propagation. The upper part of the cleaved multilayer partially shields the glue layer from the singular field at the crack tip (see [10]).

Table and Figures

	multilayer	interfacial toughness (J/m^2)
1	Glass / Si_3N_4// Ag / ZnO	0.8, 0.8, 0.9
2	Glass / Si_3N_4/ ZnO // Ag / ZnO	1.0, 1.1, 1.3
3	Glass / ZnO // Ag / ZnO	1.4, 1.6
4	Glass / TiO_2/ Ag // ZnO	1.5, 1.9, 2,8
5	Glass / SnO_2 / Ag // ZnO	2.4, 2.5

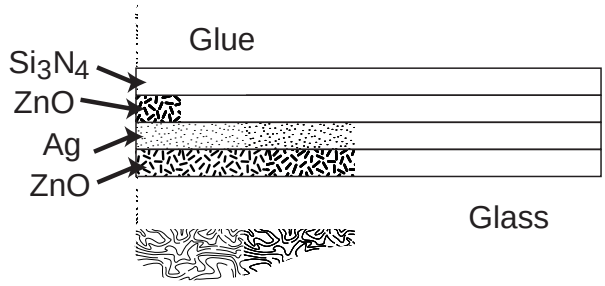

Fig. 1.

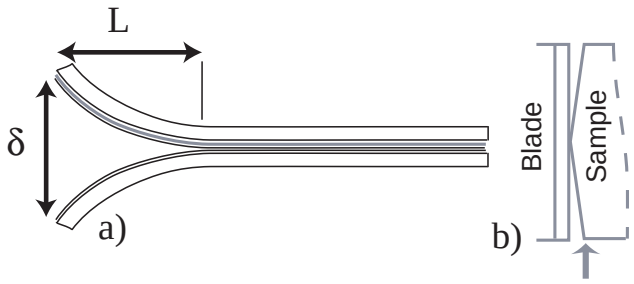

Fig. 2.

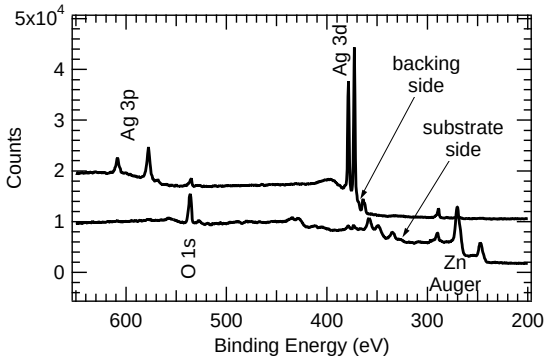

Fig. 3.

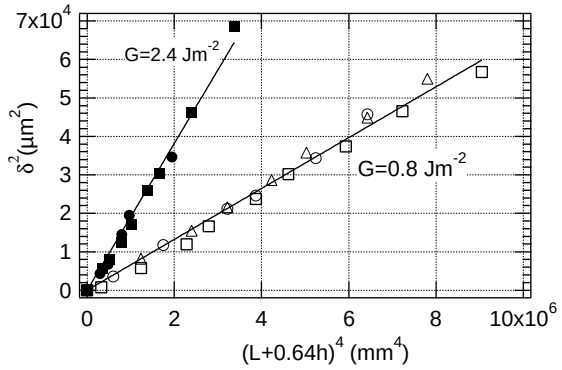
7x10^4
6
5
4
3
2
1
0
δ^2(μm^2)
G=2.4 Jm^-2
G=0.8 Jm^-2
0
2
4
6
8
10x10^6
(L+0.64h)^4 (mm^4)

Fig. 4.

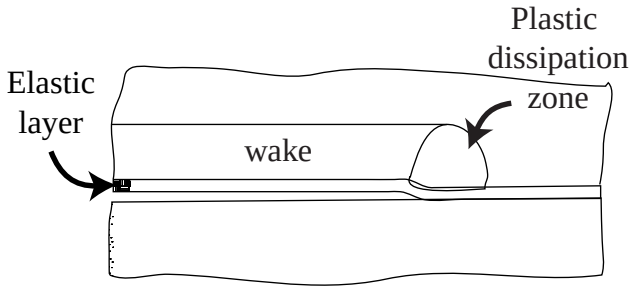
Plastic
dissipation
zone
Elastic
layer
wake

Fig. 5.